Shared developmental mechanisms pattern the vertebrate gill arch and paired fin skeletons

J. Andrew Gillis[a], Randall D. Dahn[a,1], and Neil H. Shubin[a,b]

[a]Department of Organismal Biology and Anatomy, University of Chicago, Chicago, IL 60637; and [b]The Field Museum of Natural History, Chicago, IL 60605

Edited by Clifford J. Tabin, Harvard Medical School, Boston, MA, and approved February 2, 2009 (received for review October 29, 2008)

Here, we describe the molecular patterning of chondrichthyan branchial rays (gill rays) and reveal profound developmental similarities between gill rays and vertebrate appendages. Sonic hedgehog (*Shh*) and fibroblast growth factor 8 (*Fgf8*) regulate the outgrowth and patterning of the chondrichthyan gill arch skeleton, in an interdependent manner similar to their roles in gnathostome paired appendages. Additionally, we demonstrate that paired appendages and branchial rays share other conserved developmental features, including *Shh*-mediated mirror-image duplications of the endoskeleton after exposure to retinoic acid, and *Fgf8* expression by a pseudostratified distal epithelial ridge directing endoskeletal outgrowth. These data suggest that the skeletal patterning role of the retinoic acid/*Shh*/*Fgf8* regulatory circuit has a deep evolutionary origin predating vertebrate paired appendages and may have functioned initially in patterning pharyngeal structures in a deuterostome ancestor of vertebrates.

branchial arches | development | evolution | limb | patterning

One of the most prominent hypotheses of 19th-century comparative anatomy was Gegenbaur's gill arch theory of the origin of paired appendages (1)—a hypothesis that is often contrasted to the lateral fin fold theory of Thacher (2) and Balfour (3). Gegenbaur hypothesized that paired appendages arose from modified gill arches based on the comparative anatomy of chondrichthyans (cartilaginous fishes) and osteichthyans (bony fishes). The chondrichthyan gill arch skeleton is composed of a proximal branchial arch (the epi- and ceratobranchial) and a series of distal branchial rays—fine cartilaginous rods that articulate at their bases with the branchial arch (Fig. 1 *A–C*). Gegenbaur drew parallels between the organization of the gill arch skeleton with that of the paired appendage skeletons of gnathostomes, homologizing the appendage girdle with the proximal branchial arch, and the endoskeleton of paired fins proper with the distal branchial rays. Mapping the presence of branchial ray elements on existing phylogenetic trees supports the notion that they are likely an ancestral feature of jawed fishes, as evidenced by their presence in the stem gnathostome *Euphanerops*, the stem osteichthyan *Acanthodes*, and all extant chondrichthyans (4, 5). Branchial rays (not to be confused with the gill rakers of osteichthyans) have been lost, however, in extant agnathans and osteichthyans, leaving chondrichthyans as the only organisms in which ray development might be examined and hypotheses of homology tested (6). In molecular terms, Gegenbaur's theory would predict that common mechanisms perform similar functional roles in patterning the skeletons of paired appendages and gill arch rays. To date, however, the gill arch theory has lacked supporting experimental, developmental, or molecular data. The challenge has been that no data on branchial ray development and patterning have yet been reported, in contrast to the detailed current understanding of vertebrate appendage development.

In gnathostome fin and limb buds, sonic hedgehog (*Shh*) and fibroblast growth factor (*Fgf*) cooperatively direct outgrowth and patterning of the appendage skeleton through a positive-feedback loop. *Shh* regulates anteroposterior (A/P) patterning through restricted expression by posterior mesoderm (7) and maintains *Fgf8* expression in the overlying pseudostratified apical ectodermal ridge (AER) that supports the progressive specification of skeletal elements along the proximodistal axis (8–10). FGF signaling, in turn, maintains *Shh* expression in the mesoderm (8–10). Loss of *Shh* or *Fgf8* function in developing limb buds effects a reciprocal down-regulation of *Fgf8* or *Shh* expression, respectively, with corresponding reductions in the limb skeleton (10, 11). Treatment with exogenous retinoic acid (RA) induces ectopic *Shh* expression in anterior fin/limb bud mesoderm, resulting in mirror-image duplications of skeletal elements with reversed A/P polarity (12–14).

Wall and Hogan (15) noted that *Shh* and *Fgf8* are also both expressed in the developing branchial arches of the chick, and this observation has fueled hypotheses of generative or "deep" homology of branchial arches and limbs (16, 17). Lacking in any evolutionary interpretation of the relationship between arches and limbs are gene expression or functional data from the developing gill arches—and, in particular, gill rays—of chondrichthyans. This is a crucial phylogenetic data point, given the primitive nature of chondrichthyan branchial arch morphology relative to the highly derived arches of osteichthyans (6). We therefore sought to test predictions of Gegenbaur's gill arch theory by comparatively examining the functional roles of major upstream components of the gnathostome appendage outgrowth and patterning program in the developing gill arches of a chondrichthyan, the little skate, *Leucoraja erinacea*.

Results and Discussion

Expression and Regulation of *Shh* and *Fgf8* During Gill Arch Development. We first determined that *Shh* is expressed in each of the 5 developing gill arches of the skate and is restricted to the posterior border as in tetrapod limb buds and branchial arches (Fig. 1 *D* and *E*) (7, 18). *Shh* expression spans a large developmental time frame (≈8 weeks), from the opening of the gill slits through the distal completion of gill ray chondrogenesis [stages (St.) 19–32 (19)]. In contrast to appendage buds, *Shh* is expressed by the gill arch epithelium in a continuous ridge, which overlies the distal tips of outgrowing gill rays. In parallel with appendage buds, however, *Shh* signals are received and transduced by the mesenchyme of the gill arches, as indicated by the mesenchymal expression of the *Shh* receptor gene Patched 2 (*Ptc2*) (Fig. 1*F*) (20).

Fgf8 is coexpressed by this posterior stripe of gill arch epithelium (Fig. 1*G*). Histological examination further revealed that, similar to the *Fgf8*-expressing AER of the tetrapod limb bud (10, 11), the *Fgf8*-expressing gill arch epithelium forms a pseudostratified ridge

Author contributions: J.A.G. and R.D.D. designed research; J.A.G. and R.D.D. performed research; J.A.G., R.D.D., and N.H.S. analyzed data; and J.A.G., R.D.D., and N.H.S. wrote the paper.

The authors declare no conflict of interest.

This article is a PNAS Direct Submission.

[1]To whom correspondence should be sent at the present address: Mount Desert Island Biological Laboratory, Old Bar Harbor Road, Salisbury Cove, ME 04672. E-mail: rdahn@mdibl.org.

This article contains supporting information online at www.pnas.org/cgi/content/full/0810959106/DCSupplemental.

www.pnas.org/cgi/doi/10.1073/pnas.0810959106

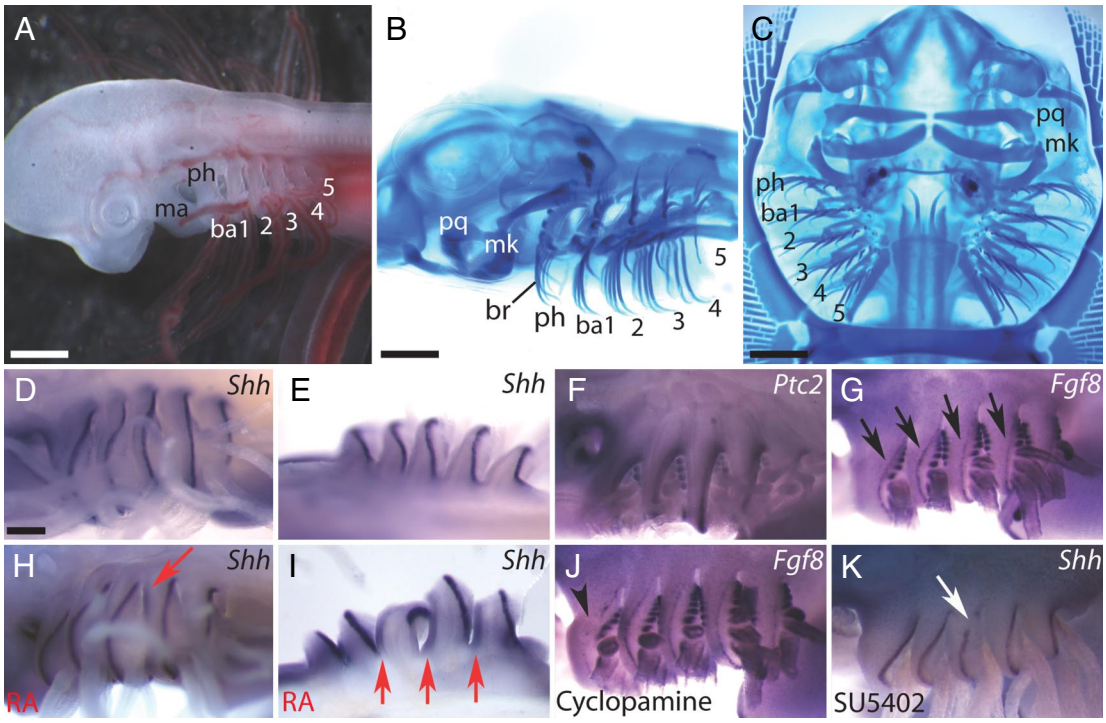

Fig. 1. Gill arch anatomy and gene expression in the embryonic skate. The 7 pharyngeal arches of embryonic skates (*A*) give rise to the serially homologous segments of the adult branchial skeleton (*B* and *C*; lateral and ventral views, respectively). The anteriormost mandibular arch (ma) forms the palatoquadrate (pq) and Meckel's cartilage (mk), whereas the 6 posterior arches develop into the pseudohyal (ph) and 5 branchial arches (ba1–5). The pseudohyal and the 4 anterior branchial arches possess branchial ray cartilages (br) that support the gill flaps; the fifth branchial arch possesses no rays. *Shh* is normally expressed by the distal ectoderm of each developing gill flap, shown in lateral (*D*) and dorsal (*E*) views, correlating with expression of the *Shh* target gene *Ptc2* in subjacent mesoderm (*F*). *Fgf8* is coexpressed by the leading edge of the gill flap epithelium (*G*, black arrows). RA treatment induces ectopic *Shh* expression (red arrows) in anterior branchial arch ectoderm (*H* and *I*; dorsal and lateral views, respectively). *Shh* and *Fgf8* function in an interdependent feedback loop: *Fgf8* is locally down-regulated by beads loaded with the SHH inhibitor cyclopamine (*J*, black arrowhead), and *Shh* expression is extinguished adjacent to beads loaded with the FGF inhibitor SU5402 (*K*, white arrow). Anterior is to the left except in *C*, where anterior is to the top. (Scale bars: *A*, 500 μm; *B* and *C*, 3 mm; *D–K*, 300 μm.)

that spans the entire leading edge of the developing gill flap (see Fig. 3 *I* and *K*). Pseudostratified ectoderm has not been observed in the branchial arches of tetrapods, which have lost branchial rays in the course of evolution. The specialized epithelium of skate branchial arches thus correlates with the retention of ray endoskeletal elements, and may reflect a functional requirement necessary for driving ray outgrowth.

We next demonstrated that *Shh* and *Fgf* signaling constitutes a functionally interdependent feedback loop in developing gill arches. The implantation of a bead loaded with the *Shh* antagonist cyclopamine (21) beneath the *Fgf8*-expressing gill epithelium resulted in localized *Fgf8* down-regulation (Fig. 1*J*) (33%, $n = 18$). Implantation of a bead loaded with the *Fgf* receptor inhibitor SU5402 (22) reciprocally down-regulated *Shh* in the overlying epithelial ridge (Fig. 1*K*) (25%, $n = 18$). Implantation of control beads never affected *Shh* or *Fgf8* expression ($n = 10$ and 12, respectively). These data identify important parallels in the signaling pathways operating in the chondrichthyan branchial arches and gnathostome appendage buds and support the hypothesis that *Shh–Fgf* feedback loops might have analogous functions in patterning the gill arch and paired fin skeletons.

RA Regulation of Gill Arch *Shh* Expression and Endoskeletal Morphology. In a further parallel with limb/fin buds, RA induces ectopic *Shh* expression in developing skate gill arches. Treatment of neurula stage embryos with exogenous RA induced ectopic *Shh* expression in the epithelium along the anterior border of gill arches (Fig. 1 *C* and *D*) (25%, $n = 20$). The ectopic anterior *Shh* expression domain is restricted to the dorsal-anterior gill arch epithelium, corresponding spatially with the epithelium overlying the epibranchial component of the gill arch endoskeleton. Although the ectopic anterior expression domain of *Shh* is less robust than the wild-type posterior-distal expression domain, it correlates with a noticeable change in external gill arch morphology (Fig. 1, compare *E* with *I*). The normal posterior domain of *Shh* expression is unaffected by RA treatment (Fig. 1 *H* and *I*), and control embryos treated with DMSO never exhibited ectopic *Shh* expression ($n = 13$).

Exogenous RA also induces mirror-image A/P duplications of the gill arch skeleton (Fig. 2 *A–H*) (70%, $n = 20$), comparable with the duplications observed in RA-treated limbs and fins (12, 14). Normally, the third branchial arch of the skate consists of 5 rays articulating with the posterior margin of the dorsal epibranchial element, 1 ray articulating at the joint between the epibranchial and ceratobranchial cartilages, and 5 rays articulating with the posterior edge of the ventral ceratobranchial cartilage; all rays curve caudally (Fig. 2 *A–D*). RA induces the formation of a supernumerary complement of branchial rays with reversed A/P polarity; ectopic rays articulate with the anterior margin of the epibranchial cartilage and curve rostrally (Fig. 2 *E–H*; Fig. S1). The normal complement of rays is unaffected by RA treatment, and ectopic rays are never observed to articulate with the posterior margin of the epi- and ceratobranchials (Fig. 2 *E–H*). Interestingly, RA-mediated duplications appear restricted to the dorsal half of the gill arch, consistent with the dorsally biased ectopic *Shh* expression induced by RA (Fig. 1 *H* and *I*); ectopic rays are never observed to articulate with the ceratobranchial cartilage (Fig. 2 *C* and *G*).

***Shh* and *Fgf8* Mediate Chondrichthyan Branchial Ray Outgrowth.** We next demonstrated that SHH signaling is sufficient to specify

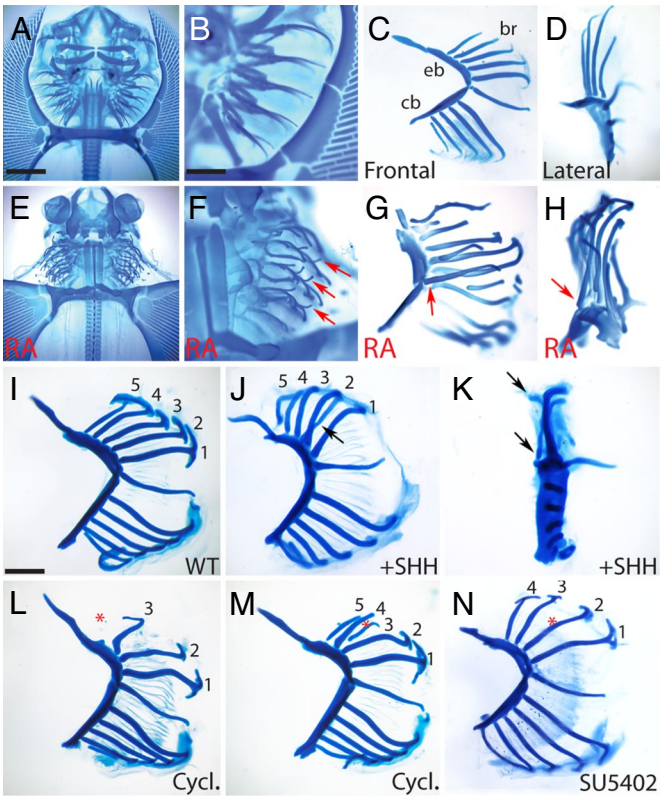

Fig. 2. RA, SHH, and FGF8 pattern the skate branchial arch skeleton. (*A–D*) Each gill arch in the skate is composed of a dorsal epibranchial (eb) and ventral ceratobranchial (cb) element that line the pharynx; branchial rays (br) articulate with the posterior border of the epi- and ceratobranchials, projecting laterally and curving caudally at the distal tip. (*E–H*) RA-treated arches exhibit mirror-image duplications of the branchial rays (red arrows); the supernumerary complement articulates with the anterior border of the epibranchial, with the distal tips curving rostrally. (*I–K*) Exogenous SHH protein can mimic RA-mediated duplications of branchial rays. (*I*) Untreated third branchial arches invariably have 5 rays articulating with the posterior margin of the epibranchial cartilage; SHH-loaded beads induce a single ectopic branchial ray (*J* and *K*), articulating with the anterior epibranchial and curving rostrally (black arrows). (*L–N*) SHH and FGF signaling are required for ray specification and outgrowth. Beads loaded with the SHH inhibitor cyclopamine (red asterisks) before ray condensation results in the complete deletion of neighboring rays (*L*), whereas postcondensation treatment results in distal ray truncations (*M*). Early treatment with the FGF antagonist SU5402 (blue asterisk) similarly results in deletion of ray cartilages. (Scale bars: *A* and *E*, 3 mm; *B–D*, *F–H*, 1.25 mm; *I–N*, 1.25 mm.)

formation and outgrowth of ectopic branchial ray cartilages. Implantation of SHH-soaked beads beneath the anterior gill arch epithelium, at stages when normal branchial rays are condensing (St. 28/29), resulted in the localized formation of a single ectopic branchial ray cartilage (Fig. 2*J* and *K*) (33%, $n = 24$). SHH-induced ectopic branchial rays articulate with the anterior margin of the epibranchial cartilage and curve rostrally (Fig. 2*K*). The similarity of SHH- and RA-induced duplications of the branchial skeleton, when considered in combination with the spatial domain of ectopic *Shh* expression in response to RA, suggest that RA's effects are mediated through SHH signaling. However, these data do not allow us to distinguish whether ectopic RA and SHH signaling are operating in linear or parallel pathways to induce ectopic rays. It has been demonstrated in the tetrapod limb that *Hox* genes—known targets of RA signaling—regulate the expression of *Shh* in the zone of polarizing activity (ZPA) (23). Epistasis experiments addressing the function of ectopic SHH in the absence of retinoids, and reciprocally, the effects of ectopic RA in the absence of SHH signaling—as well as expression analysis of putative mediators of RA regulation—are needed to fully differentiate between, and build on, these alternative hypotheses.

SHH and FGF signaling are also necessary for ray specification and outgrowth, in a manner similar to their requirements in tetrapod limbs. Cyclopamine-soaked beads implanted beneath the Shh-expressing gill arch epithelium affected ray outgrowth in a stage-dependent manner. Treatment before gill ray condensation resulted in the localized deletion of entire elements (Fig. 2*L*) (33%, $n = 18$), whereas treatment subsequent to condensation resulted in distal truncations of ray cartilages (Fig. 2*M*) (40%, $n = 10$). Similar results were observed after implantation of beads soaked in the FGF inhibitor SU5402 at comparable developmental stages (Fig. 2*N*) (25%, $n = 12$).

Conclusion

The evolutionary origin of paired appendages remains a fundamental and unresolved issue in vertebrate comparative anatomy and paleontology. More recently, this question has been reframed in evolutionary–developmental terms—under what circumstances did the paired appendage generative mechanism originate, and how has this mechanism evolved to generate morphological diversity? Gegenbaur, with his gill arch hypothesis, explicitly suggests that paired fins originated as derivations (i.e., as a transformational homologue) of a posterior, ray-bearing branchial arch (1). Implicit in this hypothesis is the postulate that ray-bearing branchial arches and paired fins descend from a common ontogenetic blueprint. It is this postulate with which we are concerned.

We have tested this postulate and demonstrated that vertebrate paired appendages and chondrichthyan branchial rays share a number of conserved regulatory and structural developmental components—the posterior bias and RA responsiveness of *Shh* expression, distal ectodermal *Fgf8* expression, and a *Shh–Fgf8* positive-feedback loop (Fig. 3). We hypothesize that these are ancestral features of gnathostome branchial arch development that functioned primitively to direct branchial ray outgrowth and that the differing expression patterns observed in osteichthyans [i.e., the restriction of *Shh* expression to arches 2 and 3 (18, 24)] are a derived condition, corresponding with the near-complete loss of lateral outgrowth—the loss of branchial rays—in these taxa. Our hypothesis rests on the notion that branchial ray-supported gills are a primitive anatomical feature of gnathostomes—a notion supported by the presence of branchial rays in all extant chondrichthyans, a stem osteichthyan, and a stem gnathostome (4, 5, 25).

Shh–Fgf feedback loops are used in the patterning of many other tissues, such as the developing brain, lungs, and genital ridge, and have long been hypothesized to be important patterning mechanisms repeatedly deployed in the evolutionary history of deuterostomes (26–28). The current work, however, provides functional data on the patterning roles of these molecular pathways in chondrichthyan branchial rays, and identifies 3 developmental properties that are uniquely shared by chondrichthyan branchial rays and vertebrate appendages: distal *Fgf8* expression by a pseudostratified epithelial ridge, the interdependent activities of *Shh* and *Fgf8* in driving and patterning endoskeletal outgrowth, and RA-induced mirror image endoskeletal duplications mediated by *Shh* signaling. These striking mechanistic similarities support our hypothesis of generative homology.

It remains to be determined whether RA and *Shh* operate in a linear genetic pathway in the branchial arches or whether RA regulates *Shh* expression via one or more intermediate pathways. It has been demonstrated in the tetrapod limb that *Hoxb6*, *Hoxb8*, and *Bmp2* exhibit modified expression patterns in the absence of retinoids (29) and that *Hox* genes function downstream of RA as regulators of *Shh* expression in the ZPA (30, 31). Misexpression of *Hoxd11–Hoxd13* in the anterior limb bud results in ectopic expres-

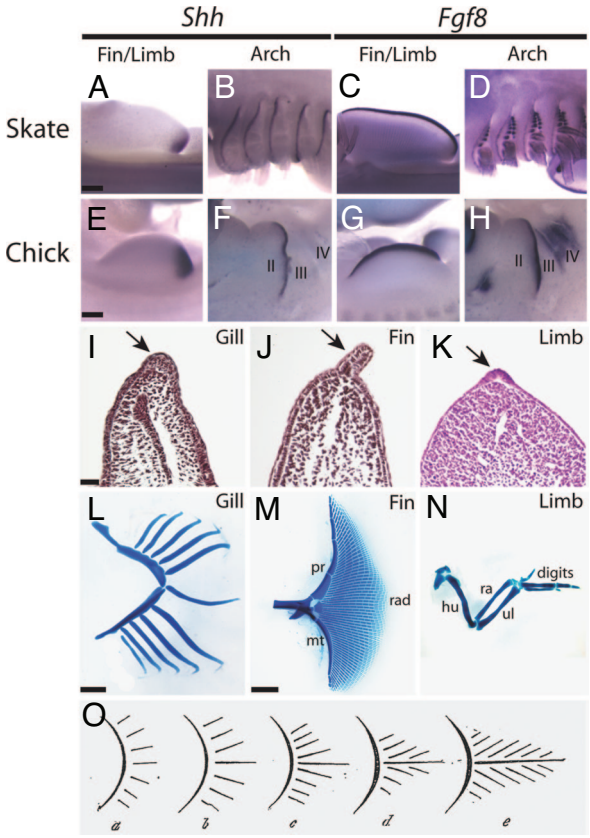

Fig. 3. Putatively homologous mechanisms regulate gnathostome appendage outgrowth. Comparative analyses of the fins and limbs of skates and chicks, and the gill arch of chondrichthyans, reveal that shared developmental signaling pathways regulate skeletal outgrowth and patterning. *Shh* expression is posteriorly restricted in the fin buds and gill arches of chondrichthyans such as the skate (*A* and *B*), as well as the limb buds and pharyngeal arches of tetrapods such as the chick (*E* and *F*). Similarly, *Fgf8* is expressed in the apical ectoderm of skate fin buds and gill arches (*C* and *D*), as well as in chick limb buds and pharyngeal arches (*G* and *H*). The structure of *Fgf8*-expressing epithelia is also conserved. Histological sections reveal that specialized pseudostratified ectodermal ridges define the distal edge of outgrowing skate gill arches (*I*), skate fin buds (*J*), and chick limb buds (*K*), and direct proximodistally complete skeletal formation (*L–N*, respectively). (*O*) The functional and regulatory conservation of molecular pathways in patterning structural outgrowths is consistent with Gegenbaur's ''Archipterygium'' hypothesis, in which he proposed that the vertebrate paired fin and gill arch skeletons are transformational homologues (*a* and *e* in *O*, respectively). pr, propterygium; mt, metapterygium; rad, radials; hu, humerus; ra, radius; ul, ulna. (Scale bars: *A–D*, 300 μm; *E–H*, 250 μm; *I–K*, 5 μm; *L*, 1.5 mm; *M*, 2 mm.)

sion of *Shh* and the induction of double posterior limbs (32), and conversely, the deletion of the HoxA and HoxD clusters results in the loss of ZPA *Shh* expression and distal endoskeletal truncations (33). *Hox* gene expression has been examined in relation to axial and appendicular patterning in a number of vertebrate species—including the shark *Scyliorhinus canicula* (34)—although with no mention of expression patterns in the developing branchial arches. Similarly, *Bmp2*, *Bmp4*, and *Bmp7* expression has been well characterized in several chordate species—and has been noted in the pharyngeal arches of *Amphioxus*, lamprey (35), *Xenopus* (36), and chick (15, 18)—although its function in branchial arch patterning has not yet been dissected. Additional studies of *Hox* and *Bmp* gene expression—and their functional roles in branchial ray morphogenesis—will no doubt provide a deeper understanding of the regulatory network patterning these structures and will potentially provide insight into how this regulatory network has evolved to generate disparate vertebrate appendage morphologies.

Although not conclusive, the functional similarities that we have described in skeletal patterning are suggestive of a generative homology of developmental mechanism between chondrichthyan branchial rays and vertebrate paired appendages, and provide experimental data consistent with Gegenbaur's hypothesized gill arch origin of vertebrate appendages. The gill arch theory would further predict a common embryonic origin of the branchial ray and fin/limb endoskeletal precursors; although neural crest contributions to the branchial arches have been demonstrated in several vertebrate species (37–39), there is no evidence for a neural crest origin of chondrichthyan gill ray cartilages (see also *Materials and Methods*). Rather, the recent demonstration that gill rays chondrify independently of the (presumably) neural crest-derived branchial arches raises the possibility that the progenitor cells of the branchial ray and fin/limb endoskeletons share a mesodermal origin (25).

The fossil record and comparative anatomy unambiguously indicate the sequential appearance of gills, median fins, and paired fins in deuterostome evolution (4–6, 40). Although the fossil record cannot unequivocally resolve the order of appearance of branchial rays and median fins, both appear before the origin of gnathostomes and paired appendages. Shared developmental gene expression patterns have previously been noted between gnathostome paired appendages and the unpaired median fins of chondrichthyans and lampreys, fueling the hypothesis that the paired fin patterning module was first assembled along the dorsal midline (41). However, the deep structural, functional, and regulatory similarities between paired appendages and the developing gill rays, and the antiquity of gills relative to appendages, allow us to suggest that the RA/*Shh*/*Fgf8* signaling network had a plesiomorphic patterning function in gills before the origin of vertebrate appendages—a function that has been retained in the gill rays of extant chondrichthyans.

Materials and Methods

Leucoraja erinacea husbandry and manipulations were performed as described in ref. 14. Windowing eggs and manipulating *L. erinacea* embryos gastrula or neurula stages invariably leads to embryo death, precluding the mapping of neural crest cell fate. Exogenous *all-trans*-RA (0.33 mg/ml in DMSO) was injected directly into egg cases to a final concentration of 1×10^{-6} M; control embryos were injected with equal volumes of DMSO alone. Embryos receiving heparin–acrylic beads soaked in mouse SHH-N (1 mg/ml; gift from Phil Beachy, Stanford University School of Medicine, Stanford, CA) or cyclopamine (4 mg/ml in DMSO; LC Laboratories), or AG-1X2 beads soaked in SU5402 (2 mg/ml in DMSO; Calbiochem), were removed from egg cases at room temperature and anesthetized in 0.64 mM Tricaine (Sigma). Embryos were placed back in their egg cases and returned to their tanks after bead implantation. Alcian blue cartilage preparations, histological processing, and expression analyses in *L. erinacea* and chick were performed as described in refs. 14 and 42. *L. erinacea* total RNA was isolated using TRIzol Reagent (Invitrogen). cDNAs were generated from total RNA using the Superscript III First Strand Synthesis System (Invitrogen), and a 3′RACE product encoding the skate *Fgf8* othologue was isolated using RT-PCR with the following forward oligonucleotides: 5′-TCAGTCCCCRCCTAATTTTACACA-3′; 5′-CCTAATTTTACACAGCATGTGAG-3′.

ACKNOWLEDGMENTS. We thank M. Davis and C. Lowe for critical discussions of the data; Marine Biological Laboratories at Woods Hole for specimens, reagents, and laboratory space; and M. Ros for reagents and a histological specimen. This work was supported by fellowships from the Natural Sciences and Engineering Research Council of Canada (J.A.G.) and the National Institutes of Health (R.D.D.), and by the Division of Biological Sciences at the University of Chicago (N.H.S.).

1. Gegenbaur C (1878) *Elements of Comparative Anatomy* (Macmillan, London).
2. Thacher JK (1877) Median and paired fins, a contribution to the history of vertebrate limbs. *Trans Conn Acad Sci* 3:281–308.
3. Balfour FM (1878) *Elasmobranch Fishes* (Macmillan, London).
4. Janvier P, Desbiens S, Willett JA, Arsenault M (2006) Lamprey-like gills in a gnathostome-related Devonian jawless vertebrate. *Nature* 440:1183–1185.

5. Nelson GJ (1968) *Current Problems of Lower Vertebrate Phylogeny*, ed Orvig T (Almqvist and Wiksell, Stockholm), pp 129–143.
6. de Beer GR (1937) *The Development of the Vertebrate Skull* (Clarendon, Oxford).
7. Riddle RD, Johnson RL, Laufer E, Tabin C (1993) Sonic hedgehog mediates the polarizing activity of the ZPA. *Cell* 75:1401–1416.
8. Laufer E, Nelson CE, Johnson RL, Morgan BA, Tabin C (1994) Sonic hedgehog and FGF-4 act through a signaling cascade and feedback loop to integrate growth and patterning of the developing limb bud. *Cell* 79:993–1003.
9. Niswander L, Jeffrey S, Martin GR, Tickle C (1994) A positive feedback loop coordinates growth and patterning in the vertebrate limb. *Nature* 371:609–612.
10. Lewandoski M, Sun X, Martin GR (2000) Fgf8 signalling from the AER is essential for normal limb development. *Nat Genet* 26:460–463.
11. Ros MA, et al. (2003) The chick *oligozeugodactyly* (*ozd*) mutant lacks sonic hedgehog function in the limb. *Development* 130:527–537.
12. Tickle C, Alberts B, Wolpert L, Lee J (1982) Local application of retinoic acid to the limb bud mimics the action of the polarizing region. *Nature* 296:564–566.
13. Akimenko MA, Ekker M (1995) Anterior duplication of the *Sonic hedgehog* expression pattern in the pectoral fin buds of zebrafish treated with retinoic acid. *Dev Biol* 170:243–247.
14. Dahn RD, Davis MC, Pappano WN, Shubin NH (2007) Sonic hedgehog function in chondrichthyan fins and the evolution of appendage patterning. *Nature* 445:311–314.
15. Wall N, Hogan B (1995) Expression of bone morphogenetic protein-4 (BMP-4), bone morphogenetic protein-7 (BMP-7), fibroblast growth factor-8 (FGF-8) and sonic hedgehog (SHH) during branchial arch development in chick. *Mech Dev* 53:383–392.
16. Shubin N, Tabin C, Carroll S (1997) Fossils, genes and the evolution of animal limbs. *Nature* 388:639–648.
17. Schneider RA, Hu D, Helms JA (1999) From head to toe: Conservation of molecular signals regulating limb and craniofacial morphogenesis. *Cell Tissue Res* 296:103–109.
18. Graham A, Okabe M, Quinlan R (2005) The role of the endoderm in the development and evolution of the pharyngeal arches. *J Anat* 207:479–487.
19. Ballard WW, Mellinger J, Lechenault H (1993) A series of normal stages for development of *Scyliorhinus canicula*, the lesser spotted dogfish (Chondrichthyes: Scyliorhinidae). *J Exp Zool* 267:318–336.
20. Pearse RV, Vogan KJ, Tabin CJ (2001) *Ptc1* and *Ptc2* transcripts provide distinct readouts of Hedgehog signaling activity during chick embryogenesis. *Dev Biol* 239:15–29.
21. Chen JK, Taipale J, Young KE, Maiti T, Beachy PA (2002) Small molecule modulation of Smoothened activity. *Proc Natl Acad Sci USA* 99:14071–14076.
22. Mohammadi M, et al. (1997) Structures of the tyrosine kinase domain of fibroblast growth factor receptor in complex with inhibitors. *Science* 276:955–960.
23. Zakany J, Duboule D (2007) The role of Hox genes during vertebrate limb development. *Curr Opin Genet Dev* 17:359–366.
24. Veitch E, et al. (1999) Pharyngeal arch patterning in the absence of neural crest. *Curr Biol* 9:1481–1484.
25. Gillis JA, Dahn RD, Shubin NH (2009) Chondrogenesis and homology of the visceral skeleton in the little skate, *Leucoraja erinacea* (Chondrichthyes: Batoidea). *J Morphol*, in press.
26. Ye W, Shimamura K, Rubenstein JL, Hynes MA, Rosenthal A (1998) FGF and Shh signals control dopaminergic and serotonergic cell fate in the anterior neural plate. *Cell* 93:755–766.
27. Lebeche D, Malpel S, Cardoso WV (1999) Fibroblast growth factor interactions in the developing lung. *Mech Dev* 86:125–136.
28. Haragichi R, et al. (2001) Unique functions of Sonic hedgehog signaling during external genitalia development. *Development* 128:4241–4250.
29. Stratford T, Logan C, Zile M, Maden M (1999) Abnormal anteroposterior and dorsoventral patterning of the limb bud in the absence of retinoids. *Mech Dev* 81:115–125.
30. Lu H-C, Revelli J-P, Goering L, Thaller C, Eichele G (1997) Retinoic signaling is required for the establishment of a ZPA and for the expression of Hoxb-8, a mediator of ZPA formation. *Development* 124:1643–1651.
31. Stratford TH, Kostakopoulou K, Maden M (1997) Hoxb-8 has a role in establishing early anterior-posterior polarity in the chick forelimb but not hindlimb. *Development* 124:4225–4234.
32. Zakany J, Kmita M, Duboule D (2004) A dual role for Hox genes in limb anterior-posterior asymmetry. *Science* 304:1669–1672.
33. Kmita M, et al. (2005) Early developmental arrest of mammalian limbs lacking HoxA/HoxD gene function. *Nature* 435:1113–1116.
34. Freitas R, Zhang G, Cohn MJ (2007) Biphasic *HoxD* gene expression in shark paired fins reveals an ancient origin of the distal limb domain. *PLoS One* 2:e754.
35. McCauley DW, Bronner-Fraser M (2004) Conservation and divergence of BMP2/4 genes in the lamprey: Expression and phylogenetic analysis suggest a single ancestral vertebrate gene. *Evol Dev* 6:411–422.
36. Hemmati-Brivanlou A, Thomsen GH (1995) Ventral mesodermal patterning in *Xenopus* embryos: Expression patterns and activities of BMP-2 and BMP-4. *Dev Genet* 17:78–89.
37. Olsson L, Hanken J (1996) Cranial neural crest migration and chondrogenic fate in the Oriental fire-bellied toad, *Bombina orientalis*: Defining the ancestral pattern of head development in anuran amphibians. *J Morphol* 229:105–120.
38. McCauley DW, Bronner-Fraser M (2003) Neural crest contributions to the lamprey head. *Development* 130:2317–2327.
39. Matsuoka T, et al. (2005) Neural crest origins of the neck and shoulder. *Nature* 436:347–355.
40. Bateson W (1886) Continued account of the later stages in the development of *Balanoglossus kowalevskii*, and of the morphology of the enteropneusta. *Q J Microsc Sci* 26:511–534.
41. Freitas R, Zhang G, Cohn M (2006) Evidence that mechanisms of fin development evolved in the midline of early vertebrates. *Nature* 442:1033–1037.
42. Dahn RD, Fallon JF (2000) Interdigital regulation of digit identity and homeotic transformation by modulated BMP signaling. *Science* 289:438–441.